

## IGR J08408–4503: A NEW RECURRENT SUPERGIANT FAST X-RAY TRANSIENT

D. GÖTZ,<sup>1</sup> M. FALANGA,<sup>1,2</sup> F. SENZIANI,<sup>3,4,5</sup> A. DE LUCA,<sup>3</sup> S. SCHANNE,<sup>1</sup> AND A. VON KIENLIN<sup>6</sup>

Received 2006 November 10; accepted 2006 December 14; published 2007 January 9

### ABSTRACT

The supergiant fast X-ray transient IGR J08408–4503 was discovered by *INTEGRAL* on 2006 May 15 during a bright flare. The source shows sporadic recurrent short bright flares, reaching a peak luminosity of  $10^{36}$  ergs  $s^{-1}$  within less than 1 hr. The companion star is HD 74194, an Ob5Ib(f) supergiant star located at 3 kpc in the Vela region. We report the light curves and broadband spectra (0.1–200 keV) of all the three flares of IGR J08408–4503 detected up to now, based on *INTEGRAL* and *Swift* data. The flare spectra are well described by a power-law model with a high-energy cutoff at  $\sim 15$  keV. The absorption column density during the flares was found to be  $\sim 10^{21}$  cm $^{-2}$ , indicating a very low matter density around the compact object. Using the supergiant donor star parameters, the wind accretion conditions imply an orbital period of the order of 1 yr, a spin period of the order of hours, and a magnetic field of the order of  $10^{13}$  G.

*Subject headings:* X-rays: binaries — X-rays: bursts — X-rays: individual (IGR J08408–4503)

### 1. INTRODUCTION

Supergiant fast X-ray transients (SFXTs), consisting of a wind-accreting compact object and an OB supergiant donor star, spend most of the time in a quiescent state, with X-ray luminosities of the order of  $10^{32}$ – $10^{33}$  ergs  $s^{-1}$ . Sporadically they go into outburst, reaching luminosities of  $10^{36}$ – $10^{37}$  ergs  $s^{-1}$  (Sguera et al. 2005; in 't Zand 2005; Negueruela et al. 2006; Smith et al. 2006). The outbursts or strong flaring activities are characterized by very short timescales, i.e., from minutes to hours. SFXTs have been discovered only recently as a new class of X-ray sources, and many unresolved fundamental questions remain open. The lack of confirmed orbital or pulse periods complicates the determination of the system parameters and the compact object nature. Up to now IGR J11215–5952 alone shows regularly recurrent outbursts every  $\sim 330$  days, most likely linked to its orbital period (Sidoli et al. 2006). To account for the accretion process that causes the short outbursts, it has been proposed that the clumpy wind in early-type stars could be captured by the compact object, producing the X-ray flares on the observed timescale (in 't Zand 2005). However, this scenario has yet to be well understood and confirmed for OB stars in binary systems.

The number of known SFXTs has grown recently thanks to the *International Gamma-Ray Astrophysics Laboratory (INTEGRAL)*; see, for example, IGR J16465–4507, IGR J17544–2619, or IGR J11215–5952 (e.g., Walter et al. 2006; Sguera et al. 2006; Sidoli et al. 2006). The new SFXT presented here, IGR J08408–4503, was discovered in the Vela region on 2006 May 15 with *INTEGRAL* during a bright outburst lasting about 15 minutes (Götz et al. 2006). The candidate optical counterpart was first tentatively identified as the supergiant, Ob5Ib(f), HD 74194 star (Götz et al. 2006; Masetti et al. 2006) located at 3 kpc in the Vela region (e.g., Walborn 1973; Humphreys 1978; Schröder et al. 2004). Subsequently, using the *Swift* X-Ray Telescope (XRT) a refined source position ( $\alpha = 08^h49^m47.97^s$  and  $\delta = -45^\circ03'29.8''$  [J2000.0])

with an uncertainty of  $5.4''$ ) was derived, strengthening the association with HD 74194 (Kennea & Campana 2006).

Optical spectra of HD 74194 measured a few days after the outburst (Barba et al. 2006) strongly resemble the ones of the companion star of another SFXT, IGR J17544–2619 (Pellizza et al. 2006). In addition, the radial velocity variations in the He I and He II absorption lines with an amplitude of about 35 km  $s^{-1}$  were measured, suggesting either a pulsating variable nature of the supergiant star HD 74194 or a possible Doppler orbital modulation (e.g., Conti et al. 1977).

IGR J08408–4503 shows the typical SFXT's recurrent short flaring events. Using *INTEGRAL* archival data, an outburst was detected on 2003 July 1 (Mereghetti et al. 2006), while the last bright flare was observed on 2006 October 4 with the *Swift* satellite (Ziaeeepour et al. 2006).

In this Letter we present the light curve and broadband spectral study of all three outbursts of IGR J08408–4503 observed up to now. In addition, thanks to the knowledge of the companion star parameters, the possible wind accretion conditions are discussed.

### 2. DATA ANALYSIS AND RESULTS

IGR J08408–4503 was observed twice in outburst with *INTEGRAL* (Winkler et al. 2003), on 2003 July 1 and 2006 May 15, i.e., during the satellite orbits 83 and 438. This data set includes publicly available data and part of AO3 Vela region guest observations. Hereafter we call the two data sets flare 1 and flare 2, respectively. We used the data from the coded mask imaging telescope IBIS/ISGRI (Ubertini et al. 2003; Lebrun et al. 2003) at energies between 15 and 200 keV and from the JEM-X monitor (Lund et al. 2003) between 3 and 20 keV. For JEM-X the data were extracted only for flare 2, flare 1 being outside the JEM-X field of view. The data reduction was performed using the standard Offline Science Analysis (OSA), version 5.1.

Single pointings ( $\sim 2000$  s each) were deconvolved and analyzed separately. The IBIS/ISGRI 15–40 keV high-energy light curve, shown in Figure 1, has been extracted from the images using all available pointings. Light curves with a 100 s time bin were also extracted around the outburst peaks.

The third outburst, flare 3, was observed on 2006 October 4 (14:45:42 UT) with the *Swift* BAT (Gehrels et al. 2004; Barthelmy et al. 2005). Since the flare was detected with an image trigger (15–150 keV), only “Survey” data products are available from the BAT instrument, with a typical integration time of  $\sim 300$  s.

<sup>1</sup> CEA Saclay, DSM/DAPNIA/Service d'Astrophysique, Gif sur Yvette, France; diego.gotz@cea.fr.

<sup>2</sup> Unité mixte de recherche Astroparticule et Cosmologie, Paris, France.

<sup>3</sup> INAF-IASF Milano, Italy.

<sup>4</sup> Université Paul Sabatier, Toulouse, France.

<sup>5</sup> Università di Pavia, Dipartimento di Fisica Nucleare e Teorica; and INFN-Pavia, Italy.

<sup>6</sup> Max-Planck-Institut für extraterrestrische Physik, Garching, Germany.

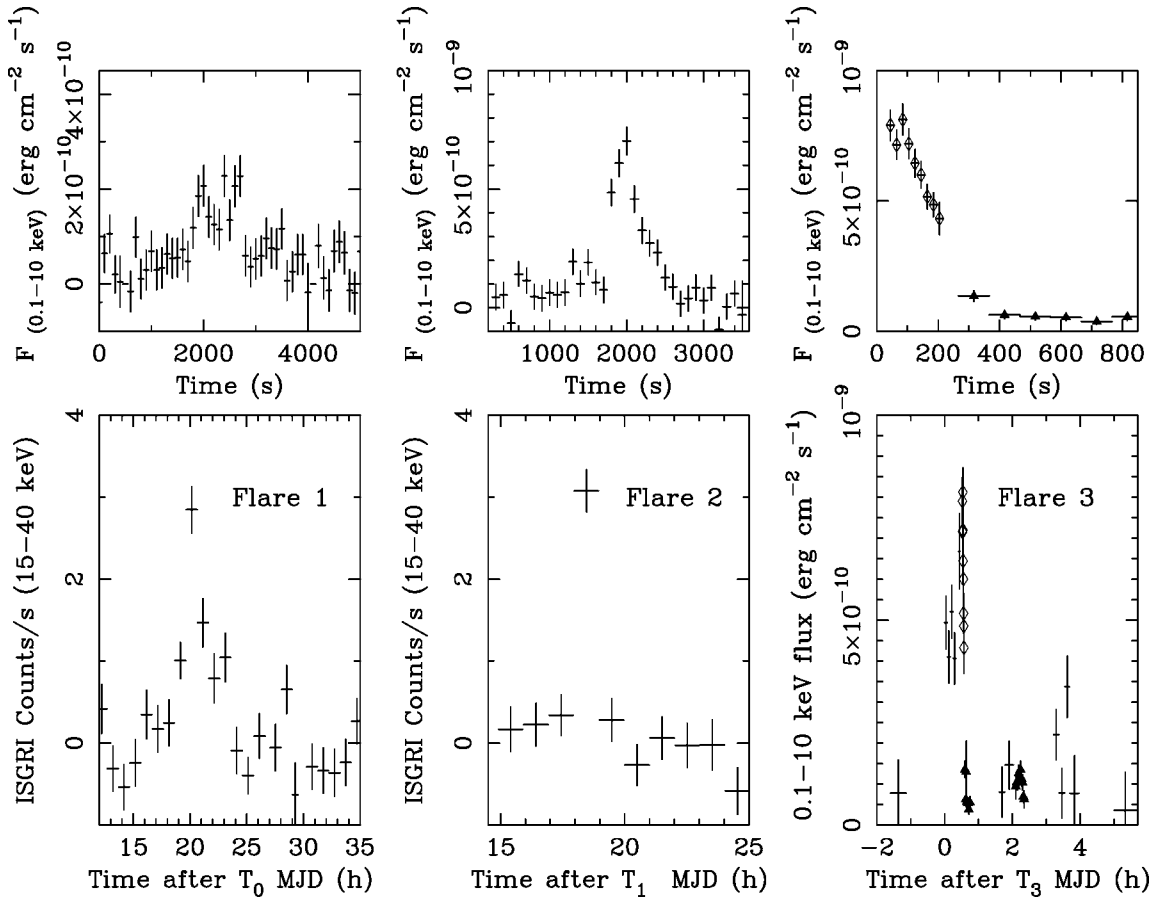


FIG. 1.—*Bottom, from left:* IBIS/ISGRI (flares 1 and 2) and *Swift* (flare 3) light curves. IBIS data are binned at  $\sim 2$  ks. In the right panel the crosses represent the extrapolated BAT flux, while the diamonds and triangles the XRT WT and PC data. The time axis is expressed in hours after  $T_0 = 52,821.0$ ,  $T_1 = 53,870.0$ , and  $T_3 = 54,012.615$  MJD, respectively. The *Swift* light curve shows also weak flares; e.g., at  $t \sim 3.5$  hr IGR J08408–4503 is detected in BAT at  $\sim 7 \sigma$  level. *Top:* The brightest part of each outburst is shown on a smaller timescale (100 s time bin for ISGRI).

We note that the BAT data coverage is not continuous due to the low Earth orbit of the *Swift* satellite. For each  $\sim 300$  s time bin the target count rate in the 14–40 keV energy range was evaluated with the mask-weighting technique using the XRT coordinates. The BAT data were selected 15 hr before and 30 hr after the trigger, and reduced using the standard software, version 2.5.

*Swift* slewed automatically to the direction of the source, and XRT (Burrows et al. 2005) (0.1–10 keV) follow-up observations were performed. The XRT data were reduced using FTOOLS version 6.1.1., and processed with XRTPIPELINE version 0.10.4, using standard filtering selections. The XRT 0.1–10 keV energy band light curves have been extracted by selecting a circular region of 20 pixels around the source for the Photon Counting (PC) mode, and a rectangular region of 40 pixels  $\times$  20 pixels for the Window Timing (WT) mode. Background light curves were extracted in source-free regions in order to produce the final background-subtracted XRT PC and WT light curves. The count rate of the source in both modes is low enough to avoid pileup in the CCD.

### 2.1. Flare Light Curves

In Figure 1 we show the three outburst light curves of IGR J08408–4503 observed up to now. The light curves are dominated by a first bright flare that typically reaches a peak luminosity of  $(3\text{--}6) \times 10^{36}$  ergs  $s^{-1}$  (see § 2.2) on a timescale of several tens of minutes to hours. The observed flares vary from an isolated strong flare (flare 2) to a more structured flaring activity (flares 1 and 3). Moreover, flare 3 shows also weaker flares with a lumi-

nosity of the order of  $5 \times 10^{35}$  ergs  $s^{-1}$ . The three outburst durations are of the order of several hours. The flare characteristics are similar to those observed in other SFXTs, such as XTE J1739–302 (e.g., Sguera et al. 2005), IGR J16465–4507 (e.g., Lutovinov et al. 2005), IGR J17544–2691 (e.g., in ’t Zand 2005), and IGR J11215–5952 (e.g., Sidoli et al. 2006), but resemble also those well studied in persistent-wind-accretion high-mass X-ray binary (HMXB) sources such as Vela X-1 (e.g., White et al. 1983) and 4U 1700–377 (e.g., Rubin et al. 1996).

Up to now only IGR J11215–5952 has shown a  $\sim 330$  day periodic outburst. Therefore, using a linear orbital function  $T(n) = T_0 + nP_{\text{orb}}$  we attempted to test the hypothesis of a periodically recurrent outburst also for IGR J08408–4503. Here  $P_{\text{orb}}$  is the orbital period in days and  $T_0$  is taken from flare 2 (MJD 53,780.771215). A possible orbital period is 4.2988 days (with  $n_1 = 244$  and  $n_2 = 33$ ); however, searching in the *INTEGRAL* archival data around the expected outburst time, we did not find any significant flux excess at the IGR J08408–4503 source position. We conclude that the three observed outbursts are sporadic episodes of accretion of matter fed from the wind of the supergiant companion star.

In order to directly compare the light curves measured with different instruments (see Fig. 1), all the count rates have been converted to the 0.1–10 keV fluxes assuming the spectral shape derived in § 2.2.

### 2.2. Flare Spectra

We performed the spectral analysis using XSPEC version 11.3, for the ISGRI data (20–200 keV) (flare 1), for the 3.5–

TABLE 1

IGR J08408–4503 SPECTRAL PARAMETERS USING A POWER-LAW MODEL WITH AN EXPONENTIAL HIGH-ENERGY CUTOFF

Data Set	Flare 1, ISGRI	Flare 2, JEM-X/ISGRI	Flare 3, XRT/BAT	Flare 4, XRT/BAT
$N_{\text{H}}^{\text{a}}$ .....	...	0.1 (fixed)	$0.1 \pm 0.03$	$<0.75$
$\Gamma$ .....	$0.0 \pm 0.5$	$0.0 \pm 0.5$	$0.1 \pm 0.2$	$0.1 \pm 0.4$
$E_{\text{c}}$ (keV) .....	$12.7 \pm 2.8$	$11.8 \pm 2.8$	$15 \pm 5$	15 (fixed)
$\chi^2/\text{dof}$ .....	14.06/12	57.09/90	80.36/75	11.72/10
$\text{Flux}_{\text{bol}}^{\text{b}}$ .....	$7.0 \times 10^{-10}$	$2.7 \times 10^{-9}$	$6.0 \times 10^{-9}$	$5.0 \times 10^{-10}$

<sup>a</sup> In units of  $10^{22} \text{ cm}^{-2}$ .<sup>b</sup> Unabsorbed 0.1–100 keV flux in units of  $\text{ergs cm}^{-2} \text{ s}^{-1}$ .

20 keV JEM-X data with the simultaneous 20–200 keV ISGRI data (flare 2), and for the 0.3–100 keV simultaneous XRT/BAT data (flare 3). Only the brightest parts of the flares have been considered. For the simultaneous data a constant factor was included in the fit to take into account the uncertainty in the cross-calibration of the instruments. All data were rebinned in order to have 3  $\sigma$  points, and the spectral uncertainties in the results are given at a 90% confidence level for a single parameter. We use a source distance of 3 kpc throughout the paper.

The XRT/BAT (flare 3) broadband (0.3–100 keV) data set provides us the widest energy coverage and the best statistics, so we fitted it first. We fitted the data using a simple photoelectrically absorbed power-law (PL) model that was found inadequate with a  $\chi^2/\text{dof} = 132.76/76$ . The addition of a high-energy exponential cutoff significantly improved the fit to  $\chi^2/\text{dof} = 80.36/75$ , resulting in a best-fit photon index of  $0.1 \pm 0.2$  and a cutoff energy at  $15 \pm 5$  keV. The hydrogen column density  $N_{\text{H}}$  was found to be  $(1.0 \pm 0.3) \times 10^{21} \text{ cm}^{-2}$ . This value is compatible with the Galactic value in the direction of the source,  $N_{\text{H}} = 3 \times 10^{21} \text{ cm}^{-2}$ , reported in the radio maps of Dickey & Lockman (1990). We attempted to fit the low-energy spectrum also with a thermal blackbody model, BB, plus a PL for the high energies, but we found a high BB temperature,  $kT_{\text{BB}} \sim 8$  keV, which is much larger than the measured values for a neutron star (NS) surface or polar cap thermal emission. Also a fit with a thermal bremsstrahlung model can be statistically ruled out by our data ( $\chi^2/\text{dof} = 183.2/76$ ). The energy spectra during the flaring activity are hence best fitted with a high-energy exponential cutoff PL model similar to the spectra observed from a persistent-wind-accreting HMXB hosting an NS, e.g., Vela X-1 (White et al. 1983).

The joint JEM-X/ISGRI (3.5–200 keV) (flare 2) spectrum was also fitted with the cutoff PL model used for flare 3. The best-fit values are similar to the ones of flare 3; see Table 1. Given that we were not able to constrain the  $N_{\text{H}}$  value (as the JEM-X bandpass starts above 3 keV), we fixed it to the value found from flare 3.

For flare 1 only ISGRI data (20–200 keV) are available. The data can be well fitted with a simple PL model with a photon index  $\Gamma$  of  $2.5 \pm 0.5$ . Note that fitting flare 2 (ISGRI) and 3 (BAT) spectra in the same energy range gives consistent photon index values, namely  $\Gamma = 2.8 \pm 0.3$  and  $2.3 \pm 0.4$ , respectively. The apparently soft spectra derived using only the data above 20 keV show how important it is to have a broad energy coverage in order to better characterize the spectrum of these sources. To be coherent, we applied the same spectral model derived from the broadband fit of flares 2 and 3 for flare 1, even if we had a smaller energy range. We fixed the slope of the power-law index to the values found (see Table 1) and found the cutoff energy compatible with the one found for flares 2 and 3.

In Figure 1 (*right*), weak flares are visible after the main peak. To infer the flux at very low mass accretion rate we extracted an XRT PC spectrum in the 0.1–6 keV energy band

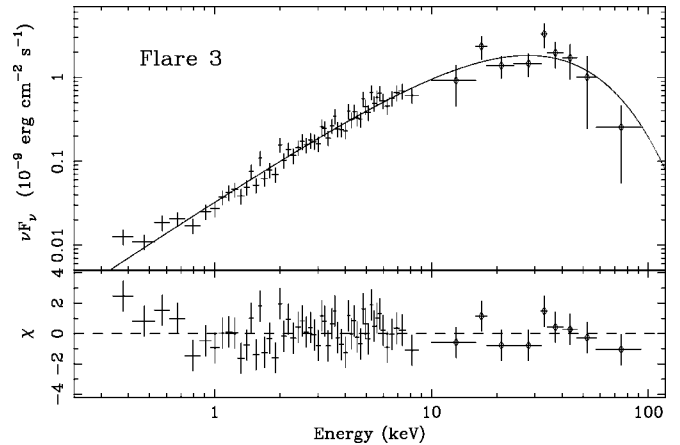


FIG. 2.—Combined XRT (*crosses*) and BAT (*diamonds*) spectra of flare 3. The best-fit PL high-energy cutoff model and the residuals (*bottom panel*) are shown.

at  $\sim 2.2$  hr after the main flare; see Figure 1. This is the last time interval where the source is clearly detected in the XRT images. We call this weak flare “flare 4.” Using the same model found for flare 3, the source was at a bolometric luminosity of  $5 \times 10^{35} \text{ ergs s}^{-1}$ , with a marginal indication of an increase of the absorption column density.

The best-fit parameters for the different flares are reported in Table 1. In Figure 2 we show the broadband unfolded spectrum and the residuals of the data to the PL with a high-energy cutoff model for flare 3.

### 3. DISCUSSION AND CONCLUSIONS

IGR J08408–4503 is a recurrent SFXT with most likely sporadic episodes of accretion of matter from the wind of the Ob51b(f), HD 74194, supergiant companion star. The broadband spectrum (0.3–200 keV) allowed us to perform an improved spectral analysis for the new source IGR J08408–4503 using XRT/BAT and JEM-X/ISGRI data. The best fit to the data required a PL with a high-energy cutoff; see Table 1. The spectrum is typical for HMXBs hosting an NS (White et al. 1983), where the emergent radiation is presumably produced by accretion columns at the magnetic poles of the NS. The bolometric flare peak luminosity is of the order of  $(3\text{--}6) \times 10^{36} \text{ ergs s}^{-1}$ , which are typical values for wind-accreting HMXBs. At low mass accretion rates, the source is observed at a bolometric luminosity of  $5 \times 10^{35} \text{ ergs s}^{-1}$ . The source quiescent luminosity is on the order of  $\sim 2 \times 10^{32} \text{ ergs s}^{-1}$  (Kennea & Campana 2006).

During the outbursts the derived absorption of  $\sim 1 \times 10^{21} \text{ cm}^{-2}$  is compatible with the total Galactic absorption in that direction as estimated from the H I maps, indicating that the source is not surrounded by large amounts of material. Some information about the distribution of matter around an X-ray binary can be inferred from observations of the variations with orbital phase of its spectrum caused by absorption along the line of sight to the X-ray star. For IGR J08408–4503 the orbital period is not known; therefore using a simply spherically symmetric stellar wind model, we approximate the wind density (e.g., see eq. [7] in Heap & Corcoran 1992) at the NS surface ( $a \gg R_*$ ;  $a$  is the binary separation) for a circular orbit:

$$N_{\text{H}} \approx 1 \times 10^{21} \left( \frac{\dot{M}_w}{10^{-7} M_{\odot} \text{ yr}^{-1}} \right) \times \left( \frac{R_*}{14.5 R_{\odot}} \right)^{-1} \left( \frac{v_{\infty}}{2000 \text{ km s}^{-1}} \right)^{-1} \text{ cm}^{-2}, \quad (1)$$

where  $\dot{M}_w$  is the HD 74194 mass-loss rate and  $v_\infty$  is the terminal wind velocity. The used stellar parameters for HD 74194 are reported in Table 2. We found the estimated  $N_H$  compatible with the derived absorption from the spectral fit. On the other hand, locating the companion star at  $a = 2R_*$  and using a maximal wind acceleration parameter  $\beta = 1$ ,  $N_H$  will change by a factor  $\ln(R_*) \approx 27$ , i.e.,  $N_H \approx 2.7 \times 10^{22} \text{ cm}^{-2}$ . The observed  $N_H$  hints at a large binary separation and therefore a large orbital period. The measured absorption is in variance with what has been observed for other SFXTs (see, e.g., Walter et al. 2006).

The companion mass loss rate  $\dot{M}_w$  was calculated for HD 74194 using the average relation for the Galactic O or B supergiants stars (Lamers & Cassinelli 1999),

$$\log(\dot{M}_w) = -1.37 + 2.07 \log(L_*/10^6) - \log(v_\infty R_*^{0.5}). \quad (2)$$

The  $\dot{M}_w$  value is a factor 10–100 lower than what is found for the persistent-wind-accretion HMXBs, such as Vela X-1 or 4U 1700–37. The free parameter to obtain a higher  $N_H$  value for IGR J08408–4503 is to have higher mass loss rates  $\dot{M}_w$ . Using equations (1) and (2) we can see that if the terminal wind velocity is a factor 5 lower (as observed for an intrinsically obscured high-energy source IGR J16318–4848 [Filliatre & Chaty 2004]), we would have a higher absorption of  $\sim 10^{23} \text{ cm}^{-2}$ , but such a low wind velocity is not observed for HD 74194. This indicates that during the accretion of matter for IGR J08408–4503 there is no accretion wake of dense matter surrounding the compact object (Blondin 1994).

We will assume that all the material within the capture radius

$$R_{\text{acc}} = \frac{2GM_x}{v_x^2 + v_\infty^2} \approx 9.2 \times 10^8 \left( \frac{\dot{M}_{\text{acc}}}{\dot{M}_w} \right)^{1/2} \left( \frac{M_* + M_x}{28 M_\odot} \right)^{1/3} P_{\text{orb}}^{1/3} \text{ cm} \quad (3)$$

is accreted by the compact object (Bondi & Hoyle 1944). Here  $M_x$  is the mass of the NS,  $v_x$  its orbital velocity, and  $\dot{M}_{\text{acc}} = L_x c^{-2} \eta^{-1}$  the mass accretion rate, where  $\eta \sim 0.2$  is the accretion efficiency for an NS. The rate of mass captured is then given by  $\dot{M}_{\text{acc}} = \dot{M}_w R_{\text{acc}}^2 / (4a^2)$ , with  $R_{\text{acc}} = 9.3 \times 10^9 \text{ cm}$ . We consider that  $v_\infty \gg v_x$  and  $a \gg R_*$ . From the measured persistent emission  $L_x \sim 2 \times 10^{32} \text{ ergs s}^{-1}$ , we derive from equation (3) an orbital period of  $\sim 1.5 \text{ yr}$ .

The condition for accretion to take place is that the NS magnetosphere radius is within the mass capture radius and the co-

TABLE 2

STELLAR PARAMETERS FOR HD 74194  
DERIVED FROM LAMERS ET AL. (1995)

Parameter	Value
$T_{\text{eff}}$ (K) .....	33000
$R_*$ ( $R_\odot$ ) .....	14.5
$M_*$ ( $M_\odot$ ) .....	28
$\log(L_*/L_\odot)$ .....	5.3
$\dot{M}_w^a$ ( $M_\odot \text{ yr}^{-1}$ ) .....	$2.3 \times 10^{-7}$
$v_\infty$ ( $\text{km s}^{-1}$ ) .....	$2000 \pm 300$
$v_{\text{esc}}$ ( $\text{km s}^{-1}$ ) .....	776

<sup>a</sup> Calculated using eq. (2).

rotation radius, i.e.,  $R_{\text{mag}} \leq R_{\text{acc}}$  and  $R_{\text{mag}} \leq R_{\text{cor}}$  (Illarionov & Sunyaev 1975). If we set  $R_{\text{acc}} = R_{\text{cor}}$  we have  $P_{\text{spin}} = 2.36 \times 10^{27} (1.4M_x)v_\infty^{-3} \approx 7000 \text{ s}$ . The magnetosphere radius is given by

$$R_{\text{mag}} = 0.1 \mu^{1/3} \dot{M}_w^{1/6} v_\infty^{-1/6} M_*^{1/9} P_{\text{orb}}^{2/9}, \quad (4)$$

where  $\mu = BR_{\text{NS}}^3$ . Setting the accretion condition  $R_{\text{mag}} = R_{\text{cor}} = R_{\text{acc}}$  the magnetic field has to be  $B \sim 1.1 \times 10^{13} (P_{\text{orb}}/1 \text{ yr})^{-2/3} \text{ G}$ , for  $R_{\text{NS}} = 10^6 \text{ cm}$ . Assuming the orbital period derived above, the NS magnetic field has to be of the order of  $10^{13} \text{ G}$ . These are typical magnetic field values for young HMXBs hosting an NS, such as Vela X-1 (La Barbera et al. 2003).

The low  $N_H$  value measured during the flares is not consistent with the picture in which they are caused by clumps in the donor wind. In an alternative scenario, the flares could be associated with the sudden accretion onto the magnetic poles of matter previously stored in the magnetosphere during the quiescent phase. However, in order to have such a mass storage, the above simplest accretion conditions have to be studied for different scenarios (e.g.,  $R_{\text{acc}} > R_{\text{cor}} > R_{\text{mag}}$ ). One can derive these conditions by varying opportunely  $P_{\text{orb}}$ ,  $P_{\text{spin}}$ , and  $B$  (E. Bozzo et al. 2007, in preparation).

We conclude that these recurrent sporadic very short outburst episodes, due to the accretion of matter from the wind of a supergiant companion star, imply a spin period of the order of hours with a long orbital period, and a  $10^{13} \text{ G}$  magnetic field for the NS. The determination of all the system parameters can help to solve the accretion mechanism.

D. G. and M. F. acknowledge the French Space Agency (CNES) for financial support. M. F. is grateful to Luigi Stella and Enrico Bozzo for helpful discussions during his visit in Rome. A. D. L. acknowledges an ASI fellowship.

## REFERENCES

- Barba, R., Gamen, R., & Morrell, N. 2006, *Astron. Tel.*, 819, 1  
 Barthelmy, S. D., et al. 2005, *Space Sci. Rev.*, 120, 143  
 Blondin, J., M. 1994, *ApJ*, 435, 756  
 Bondi, H., & Hoyle, F. 1944, *MNRAS*, 104, 273  
 Burrows, D. N., et al. 2005, *Space Sci. Rev.*, 120, 165  
 Conti, P. S., Leep, E. M., & Lorre, J. J. 1977, *ApJ*, 214, 759  
 Dickey, J. M., & Lockman, F. J. 1990, *ARA&A*, 28, 215  
 Filliatre, P., & Chaty, S. 2004, *ApJ*, 616, 469  
 Gehrels, N., et al. 2004, *ApJ*, 611, 1005  
 Götz, D., et al. 2006, *Astron. Tel.*, 813, 1  
 Heap, S. R., & Corcoran, M. F. 1992, *ApJ*, 387, 340  
 Humphreys, R. M. 1978, *ApJS*, 38, 309  
 Illarionov, A., & Sunyaev, R. 1975, *A&A*, 39, 185  
 in 't Zand, J. J. M. 2005, *A&A*, 441, L1  
 Kennea, J. A., & Campana, S. 2006, *Astron. Tel.*, 818, 1  
 La Barbera, A., et al. 2003, *A&A*, 400, 993  
 Lamers, H. J. G. L. M., & Cassinelli, J. P. 1999, *Introduction to Stellar Winds* (Cambridge: Cambridge Univ. Press)  
 Lamers, H. J. G. L. M., Snow, T. P., & Lindholm, D. M. 1995, *ApJ*, 455, 269  
 Lebrun, F., et al. 2003, *A&A*, 411, L141  
 Lund, N., et al. 2003, *A&A*, 411, L231  
 Lutovinov, A., et al. 2005, *A&A*, 444, 821  
 Masetti, N., et al. 2006, *Astron. Tel.*, 815, 1  
 Mereghetti, S., Sidoli, L., Paizis, A., & Götz, D. 2006, *Astron. Tel.*, 814, 1  
 Negueruela, I., et al. 2006, *ApJ*, 638, 982  
 Pellizza, L. J., Chaty, S., & Negueruela, I. 2006, *A&A*, 455, 653  
 Rubin, B., C., Finger, M. H., & Harmon, B. A. 1996, *ApJ*, 459, 259  
 Schröder, S. E., et al. 2004, *A&A*, 428, 149  
 Sguera, V., et al. 2005, *A&A*, 444, 221  
 ———. 2006, *ApJ*, 646, 452  
 Sidoli, L., Paizis, A., & Mereghetti, S. 2006, *A&A*, 450, L9  
 Smith, D. M., et al. 2006, *ApJ*, 638, 974  
 Ubertini, P., et al. 2003, *A&A*, 411, L131  
 Walborn, N. R. 1973, *AJ*, 78, 1067  
 Walter, R., et al. 2006, *A&A*, 453, 133  
 White, N. E., Swank, J. H., & Holt, S. S. 1983, *ApJ*, 270, 711  
 Winkler, C., et al. 2003, *A&A*, 411, L1  
 Ziaeeipour, H., et al. 2006, *GCN Circ.* 5687, <http://gcn.gsfc.nasa.gov/gcn/gcn3/5687.gcn3>